Available online at www.sciencedirect.com

ScienceDirect

Procedia Structural Integrity 13 (2018) 1460–1469

Structural Integrity Procedia

www.elsevier.com/locate/procedia

ECF22 - Loading and Environmental effects on Structural Integrity

Modelling of hyperelastic polymers for automotive lamps under random vibration loading with proportional damping for robust fatigue analysis

C P Okeke[a,b]*, A N Thite[a], J F Durodola[a], N A Fellows[a] and M T Greenrod[b]

[a] *Department of Mechanical Engineering and Mathematical Sciences, Oxford Brookes University, Oxford – OX33 1HX, UK*

[b] *Wipac Ltd, London Road, Buckingham, MK18 1BH, UK*

Abstract

The objective of this paper was to model random vibration response of components of an automotive lamp made of Polycarbonate/Acrylonitrile Butadiene Styrene (PC-ABS), Polymethyl methacrylate (PMMA) and Polypropylene 40% Talc filled (PPT40) materials using a nonlinear hyperelastic model. Traditionally, the Rayleigh damping matrix used in the dynamic response analysis is constructed considering linear elastic behaviour based on either initial stiffness or secant stiffness. The performance of linear stiffness matrices is compared in this work with that based on the nonlinear hyperelastic, Mooney-Rivlin model, specifically addressing Rayleigh damping matrix construction. The random vibration responses of 10 samples of each material are measured. The mean square error of acceleration response was used to assess the effectiveness. Considering three materials of study, the hyperelastic model resulted in the reduction of the least square error at best by 11.8 times and at worst by 2.6 times. The Mooney-Rivlin material model based Raleigh damping matrix was more accurate in modelling the dynamic behaviour of components of nonlinear materials and it also represented the manufacturing variabilities more reliably.

Peer-review under responsibility of the ECF22 organizers.

Keywords: Hyperelastic; Mooney_Rivlin, material models; nonlinear stress-strain; simulation; modelling; proportional damping; rayleigh; transient analysis; random vibration; manufacturing variations

1. Introduction

Polymers are now materials of choice in the construction of automotive lamps due to their good mechanical and optical properties, light weight and design flexibility. However, modelling dynamic response of polymers for fatigue

* Corresponding author. Tel.: +44-(0)1865-423011
E-mail address: c.okeke100@gmail.com; 14101309@brookes.ac.uk

2452-3216
Peer-review under responsibility of the ECF22 organizers.
10.1016/j.prostr.2018.12.302

analysis can be demanding and complex, as their properties are severely influenced by their molecular structures, environmental condition and the method of manufacturing. The complexities increase if non-linear models are to be used. Polymers exhibit hyperelastic behaviour under deformation. The numerical simulation of the dynamic response of nonlinear elastic structures using hyperelastic material models can only be performed in transient mode, an analysis performed in the time domain. This analysis is computationally intensive compared to the traditional frequency domain approach but it offers an advantage of visualising the behaviour of a structure in real time along with appropriate considerations for nonlinearities.

In the numerical modelling of dynamic behaviour of structures, damping plays an important role in influencing the peak amplitudes. Rayleigh damping model is often used Nakamura (2016). The Rayleigh damping model comprises viscous and material or hysteresis damping components (alpha and beta). The damping matrix is proportional to the mass matrix and stiffness matrix. Traditionally, the damping matrix is constructed using linear model based stiffness, either using initial tensile stiffness or secant stiffness. The damping matrix based on linear model does not take into account the material nonlinearity as the stiffness is assumed to be constant for the entire elastic region. This may introduce errors in the analysis of a structure with nonlinear elastic materials such as polymers. This problem has been noted by Bernal (1994) and Zareian et al. (2010). Charney (2008) and Jehel et al. (2013) also presented the same view and suggest using tangent modulus based stiffness instead of initial tensile modulus. However, constructing damping matrix with tangent stiffness may still generate error in the dynamic response of a nonlinear system.

In this study, the random vibration response of PC-ABS, PMMA and PPT40 materials of automotive lamp was modelled using nonlinear hyperelastic material model based stiffness damping matrix and the results compared with those based on traditional linear model of initial stiffness and secant stiffness damping matrices. The Mooney-Rivlin and linear models parameters of the three materials were obtained from uniaxial tension experimental data measured using non-contact video gauge. Ten samples each were tested to evaluate the effect of manufacturing variability. The proportional damping coefficients were obtained from damping ratios estimated using half power bandwidth method. A full transient simulation was performed using nonlinear Mooney-Rivlin stiffness based damping matrix and linear initial tensile and secant stiffness damping matrices. The corresponding acceleration responses were compared to the experimentally obtained acceleration response using a vibration shaker. The statistics of the acceleration response for Mooney-Rivlin based damping matrix were obtained from the simulation of ten specimens to measure the inter-sample variation due to manufacturing process.

2. Random vibration response analysis

The base excited, randomly vibrating structure's response can be written as:

$$[M]\{\ddot{X}\} + [C]\{\dot{X}\} + [K]\{X\} = F - \{m\ddot{y}\} \quad (1)$$

where $\{X\}$, $\{\dot{X}\}$ and $\{\ddot{X}\}$ are nodal displacement nodal velocity and nodal acceleration vectors respectively. $[M]$, $[C]$ and $[K]$ are mass, damping and stiffness matrices and m is mass of the base and $\ddot{y}$ is a random acceleration input. The stiffness and damping matrices on the left hand of the equation play major roles in the system behaviour and therefore need to be clearly defined.

2.1. Stiffness matrix

The linear stiffness has been widely used in modelling the response of a structure subjected to external loading. However, with a high level of non-linearity in polymers, large errors may occur if linear stiffness model are used. The non-linear elastic behaviour of polymers can be modelled using hyperplastic model. Here, nonlinear material model of hyperelastic and linear material models are described. The elastic modulus which is a measure of stiffness is captured at every point of the curve for hyperelastic model but for linear model only one value of modulus is obtained, which can be either elastic modulus or tensile modulus.

2.2. Hyperelastic material model

The hyperelastic models can be of phenomenological and micromechanical type. The stress-strain relationship for hyperelastic material is generally obtained from a strain energy density function, which is normally denoted as W; stress is obtained as a first derivative of the strain energy density function and with respect to strain:

$$\sigma_{ij} = \frac{\partial W}{\partial E_{ij}} \tag{2}$$

For incompressible materials, the strain energy density function is dependent on the stretch invariants $I_{1,2}$. The stretch invariants are given by: $I_1 = \lambda_1^2 + \lambda_2^2 + \lambda_3^2$ and $I_2 = \lambda_1^2\lambda_2^2 + \lambda_2^2\lambda_3^2 + \lambda_3^2\lambda_1^2$. The principal stretch ratios ($\lambda_{1,2,3}$) are obtained from the transformation of principal axis, and for uniaxial tension they are:

$$\lambda_1 = \lambda = \frac{L}{L_o}; \quad \lambda_2 = \lambda_3 = \frac{1}{\sqrt{\lambda}} \tag{3}$$

It is shown in Okeke et al. (2017) that Mooney-Rivlin model, Mooney (1940), Rivlin (1948), which is of a phenomenological type, represents the elastic behaviour of polymer materials robustly. The order of the model can be varied depending on the magnitude of the exhibited non-linearity. In this study three parameter Mooney-Rivlin model was used to model the mechanical behaviours of PC-ABS and PMMA materials while five parameter model was used for PPT40 material. The uniaxial stress expressions for incompressible material for three and five parameter Mooney-Rivlin model are given below Kumar et al. (2016), Nowark (2008):

3 – Parameters:

$$\sigma_{3p} = 2C_{10}\left(\lambda - \frac{1}{\lambda}\right) + 2C_{01}\left(1 - \frac{1}{\lambda^3}\right) + 6C_{11}(\lambda^2 - \lambda - 1 + \frac{1}{\lambda^2} + \frac{1}{\lambda^3} - \frac{1}{\lambda^4} \tag{4}$$

5 – Parameters:

$$\sigma_{5p} = 2C_{10}\left(\lambda - \frac{1}{\lambda}\right) + 2C_{01}\left(1 - \frac{1}{\lambda^3}\right) + 6C_{11}\left(\lambda^2 - \lambda - 1 + \frac{1}{\lambda^2} + \frac{1}{\lambda^3} - \frac{1}{\lambda^4}\right) + 4C_{20}\lambda\left(1 - \frac{1}{\lambda^3}\right)\left(\lambda^2 + \frac{2}{\lambda} - 3\right) + 4C_{02}\left(2\lambda + \frac{1}{\lambda^2} - 3\right)\left(1 - \frac{1}{\lambda^3}\right) \tag{5}$$

The material constants $C_{10}, C_{01}, C_{11}, C_{20},$ and C_{02} are determined from the experimental data.

2.3. Linear elastic model

The principle of linear elastic model is that the stress is proportional to strain and the deformation resulting from the applied load is small. This model is grounded on Hooke's law of isotropic elasticity. The ratio of stress to the corresponding strain known as elastic modulus (E) and the ratio of transverse strain to longitudinal strain known as Poisson's ratio ($\boldsymbol{\upsilon}$) are the two basic elastic parameters required for linear elastic model. When there is no proportionality between the stress and the strain within the elastic limit, the standards ASTM (D638-02), recommends the use of secant modulus in the linear model instead of elastic modulus. The secant modulus is defined as the ratio of the nominal stress to corresponding strain at any chosen point on the stress-strain curve. The equations for the linear and secant modulus are given below in equation (6):

$$E_t = \frac{\sigma_2 - \sigma_1}{\varepsilon_2 - \varepsilon_1}, \quad E_s = \frac{\sigma}{\varepsilon} \tag{6}$$

2.4. Damping matrix

The damping matric is expressed as:

$$[C] = \alpha[M] + \beta[K] \tag{7}$$

where alpha (α) and beta (β) are Rayleigh damping components. Alpha (α) represents the viscous damping element and beta (β) represents the material or hysteresis damping element. Both Rayleigh components can be obtained from the following systems of equations:

$$\alpha + \beta\omega_1^2 = 2\omega_1\zeta_1\,, \qquad \alpha + \beta\omega_2^2 = 2\omega_2\zeta_2 \tag{8}$$

here ζ and ω are the damping ratio and the corresponding natural frequency. The damping properties can be estimated using the first two modes of vibration. The Rayleigh damping components based on first two modes of vibration are described by the equations:

$$\alpha = 2\omega_1\omega_2\frac{\zeta_1\omega_2 - \zeta_2\omega_1}{\omega_2^2 - \omega_1^2},\ \ \beta = 2\frac{\zeta_2\omega_2 - \zeta_1\omega_1}{\omega_2^2 - \omega_1^2} \tag{9}$$

The Rayleigh damping constants alpha (α) and beta (β) can be used to generate three damping matrices based on the material models. For linear model based damping matrix of equation (6) using initial tensile stiffness and tensile stiffness, we have:

$$[C] = \alpha[M] + \beta[K]_{E_t=\frac{\sigma_{2-\sigma_1}}{\varepsilon_{2-\varepsilon_1}}},\ \ [C] = \alpha[M] + \beta[K]_{E_s=\frac{\sigma}{\varepsilon}rp} \tag{10}$$

For nonlinear Mooney-Rivlin model damping matrix is given by:

$$[C] = \alpha[M] + \beta[K]_{\partial E_{ij}=\frac{\partial W}{\sigma_{ij}}} \tag{11}$$

3. Experimental

3.1. Tensile testing

The PC-ABS and PPT40 test specimens were standard A1 injection moulded dumb bell tensile specimens supplied by manufacturers Albis and Plastribution respectively. The dimensions were in line with the recommendation in the test standard BS EN ISO (527-2). Apart from the PMMA, the dimensions of all the tested samples of the materials were 170mm x 10mm x 4mm. For the PMMA material, dog bone shaped specimens were cut out from an optical plate that was injection moulded at Wipac. The dimensions of the narrow parallel sided portion were 80mm x 10mm x 3mm. The tensile testing was performed under room temperature using Instron 5582 tensile test machine. A constant crosshead speed of 1mm/min was used to pull the samples to failure. The strain was determined using non-contact video gauge. Ten specimens for each of the materials were tested.

3.2. Random Vibration testing

The random vibration test was performed under room temperature using LDS V721 vibration shaker. The shaker was driven by LDS 5KVA Spak Power Amplifier, and controlled with LDS laser USB controller. The test profile was based on ISO (16750-3) specification. The value of the root mean square (RMS) of the random vibration acceleration profile was 27.8m/s^2 and the frequency range was of 10 to 1000Hz. The test specimen was mounted on a test fixture in a cantilever arrangement. The control and response accelerometers used were PCB Piezotronics 353B03 and 352C22 miniature respectively.

3.3. Damping test

The damping test was performed by a sine sweep input from 5 to 1000Hz frequency range and a constant input acceleration of 1g. Five specimens for each of the materials were tested. The test set-up was the same as the random vibration test in section 3.2. Since the resonance frequencies were well separated, the half power bandwidth method was used to estimate the modal damping ratios.

4. Finite element simulation

The random vibration response analysis of a system with nonlinear material can only be carried out in transient mode. In this study, a full transient simulation was performed using ANSYS workbench to validate the dynamic response of PC-ABS, PMMA and PPT40 polymers subjected to random vibration loading. Parameters of each of the ten specimens characterised with both linear and non-linear models were simulated to validate the inter-sample variations in the responses. The random vibration input loading of the specification ISO (16750-3) was converted from frequency domain to time domain using electrodynamic vibration shaker. A large mass was added to the base of the specimens to facilitate the base excitation of the system which was a cantilever beam arrangement. The added large mass was used to convert the input acceleration spectrum to an input force spectrum in order to avoid the undesirable results from the mass proportional damping (alpha). Fig 1 shows the schematic diagram of the test arrangement. *F* is the shaker force required to achieve appropriate level of imposed base acceleration.

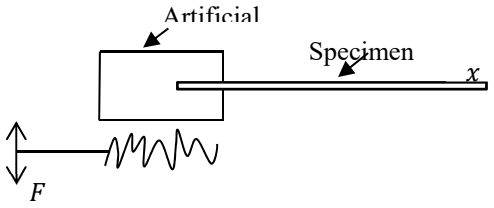

Figure 1: Schematic diagram of the model set-up

5. Results and discussion

5.1. Stress-strain curves

The stress-strain curves of PC-ABS, PMMA and PPT40 materials are shown in fig 2. The curves represent 90% yield stress of the materials. In practice, the yield stress of 80% to 90% material is adopted as the safe design stress in the engineering applications. The yield stress of the materials averaged over ten specimens tested was 53MPa for PC-ABS, 62MPa for PMMA and 28MPa for PPT40. It can be observed from the plots that the stress-strain curves of the three materials show nonlinearity up to the elastic peak stress (elastic limit). This nonlinearity appears to be largest in PPT40 followed by PMMA material. The nonlinear behaviour in the elastic region resulted in the variation of the elastic properties. The stiffness of these materials varied and the rate of variation can be significant depending on the level of the strain experienced by the materials when subjected to external loading. Another important aspect to note here is inter-sample variations, which were due to the manufacturing process. There were significant inter-sample variations in PPT40 material, and PC-ABS and PMMA also showed inter-sample variations but to lesser degree. This observed nonlinearity and the inter-sample variations need to be taken into account when these materials are used in construction of engineering structures.

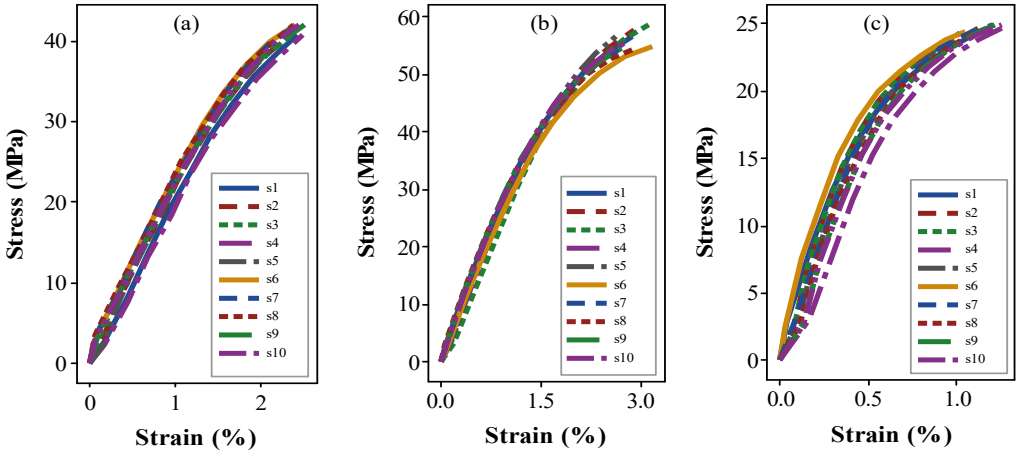

Figure 2: Stress-strain curves - (a) PC-ABS, (b) PMMA, (c) PPT40

5.2. Hyperelastic material model parameters

The Mooney-Rivlin model parameters were derived from the experimental data using MATLAB. The material model parameters were obtained from ten specimens for each of the three materials. Statistical analysis was performed on the parameters obtained in order to understand the measure of variation. The statistical results for the Mooney-Rivlin model parameters are given in Table 1. The result shows that the C_{01} parameter of 3-parameter Mooney-Rivlin for PC-ABS and PMMA exhibits higher deviation from the mean when compared to C_{10} and C_{11} parameters. The C_{01} parameter has a significant influence on the level of material nonlinearity, the larger the C_{01} the larger the nonlinearity in the material. Overall, the standard deviation is higher for the PC-ABS when compared to PMMA material. The 5-parameter model used for the PPT40 material shows higher standard deviation when compared to the 3-parameter used for the other two materials.

Table 1: Hyperelastic material model parameters

Constants	PC-ABS		PMMA		PPT40	
	Mean	Standard deviation	Mean	Standard deviation	Mean	Standard deviation
C_{10}	11.340	0.956	14.812	1.014	53.300	59.700
C_{01}	-4.507	1.987	-5.688	2.215	-36.300	52.400
C_{11}	-0.452	0.067	-0.648	0.039	-4.300	141.200
C_{20}	-	-	-	-	8.800	202.900
C_{02}	-	-	-	-	-23.100	89.200

The mean values of the model parameters obtained were used to construct average stress-strain curve and compared to the mean experimental stress and the plots are shown in fig 3. Mooney-Rivlin 3-paramter model for PC-ABS and PMMA materials shows good agreement with the experiment, while 5-parameter for PPT40 closely follows the experimental curve but not as good as the other two materials. Overall, it is evident that Mooney-Rivlin model gives a good representation of the elastic behaviour of polymers.

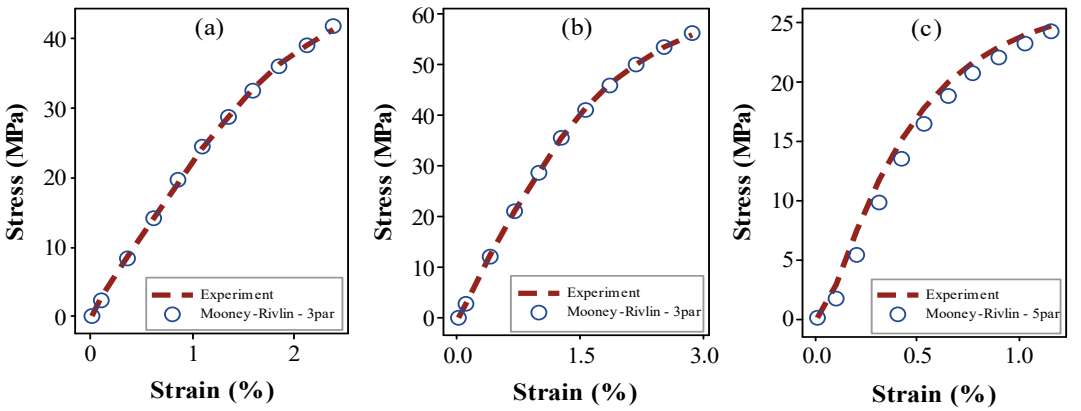

Figure 3: Stress-strain curves - experiment and models - (a) PC-ABS, (b) PMMA, (c) PPT40

5.3. Linear material model parameters

The linear model parameters were obtained from ten specimens for each of the materials in accordance to the standards (BS EN ISO 525-2, ASTM D638-02a). Statistical analysis was performed on the models parameters obtained to understand the statistical measure of variation. The parameters of the linear elastic models in table 2 show minimal standard variation for all the materials. For tensile stress, PMMA shows 2.7% standard deviation which is the largest when compared to 0.3% and 0.6% of PC-ABS and PPT40 materials respectively. For the initial tensile modulus, PPT40 material has 16% standard deviation which is the largest when compared to 15.8 and 5% for PC-ABS and PMMA materials. For secant modulus and Poisson's ratio, again PPT40 standard deviations are higher, 7.3% and 25% respectively, while PMMA has 6% and 18%, and PC-ABS has the least of 2.3% and 16%.

Table 2: Linear elastic model parameters

	PC-ABS		PMMA		PPT40	
	Mean	Standard deviation	Mean	Standard deviation	Mean	Standard deviation
Initial Tensile Modulus (MPa)	2269.000	359.000	3209.900	163.100	4853.000	782.000
Secant Modulus (MPa)	1733.100	40.400	1967.300	121.400	2142.900	155.800
Poisson's ratio	0.398	0.063	0.448	0.080	0.348	0.087

5.4. Damping

The damping ratios based on five specimens were obtained from two dominants vibration modes using half power bandwidth method. The values of the damping ratios were used to calculate Rayleigh damping constants and the statistics were measured. Table 3 lists the statistics of the Rayleigh damping constants. The standard deviation of alpha

and beta of PC-ABS material were 1% and 18% respectively. For PMMA material, standard deviations of alpha and beta were 11% and 33% respectively. In the case of PPT40 material, the standard deviation of the mean for alpha and beta are 16% and 10% respectively. The mean values of the Rayleigh components were used to construct the damping matrix to assess the behaviour of these materials under random vibration loading.

Table 3: Rayleigh damping constants based on tests of five specimens

	PC-ABS		PMMA		PPT40	
Constants	Mean	Standard deviation	Mean	Standard deviation	Mean	Standard deviation
Beta (β)	3.27E-06	5.9407E-07	3.53E-05	1.16935E-05	2.06E-05	2.06007E-06
Alpha (α)	10.539	0.114	18.672	2.040	23.207	3.746

6. Simulation results

6.1. Responses - Hyperelastic versus linear elastic of initial and secant based stiffness

Modelling the dynamic response of a system with nonlinear material requires the use of nonlinear hyperelastic material model. However, linear elastic model has normally been used for this type of problem Jehel et al (2014). Here the stiffness part of damping matrix was constructed with hyperelastic material model based stiffness and linear elastic model of initial and secant based stiffness and the dynamic response results of these models are compared with the experimental result. The material parameters used to model the random responses for both linear and nonlinear were the mean values obtained over ten specimens. Fig 4 shows the acceleration responses of PC-ABS material for the three models studied, (a) hyperelastic stiffness based damping matrix, (b) initial stiffness based damping matrix and (c) secant stiffness based damping matrix. The response curve of the hyperelastic Mooney-Rivlin model was in better agreement with the experimental response curve than that of linear models of initial stiffness and secant stiffness models; this was also true for PMMA and PPT40 materials. The mean square error of acceleration response was compared to the experimental response for the models of all the three materials as shown in fig 5. It can be seen that the mean square error of acceleration for the hyperelastic material model is the least for all the materials. For PC-ABS material, the mean square error for hyperelastic material model was 0.7(m^2/s^4), the corresponding values for linear elastic models of initial tensile modulus and the secant modulus were 8.3(m^2/s^4) and 6.2(m^2/s^4). For the PPT40 material, the hyperelastic model had a mean square error of 1.06(m^2/s^4) and the corresponding values for linear elastic models of initial tensile modulus and the secant modulus were 4.1(m^2/s^4) and 2.2(m^2/s^4) respectively. In the case of PMMA material, the mean square error of hyperelastic material model was 0.62(m^2/s^4), the linear elastic models of initial tensile modulus and the secant modulus are 4.2$(m/s^2)^2$ and 2.8(m^2/s^4), much higher than for hyperelastic model.

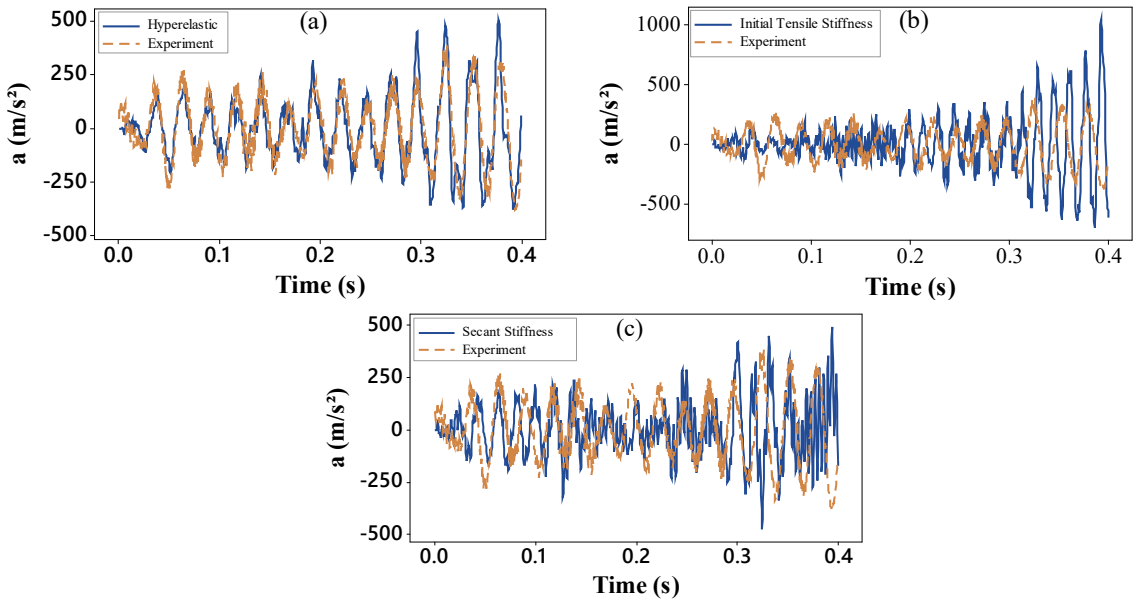

Figure 4: Response acceleration- PC-ABS - (a) hyperelastic, (b) initial tensile stiffness, (c) secant stiffness

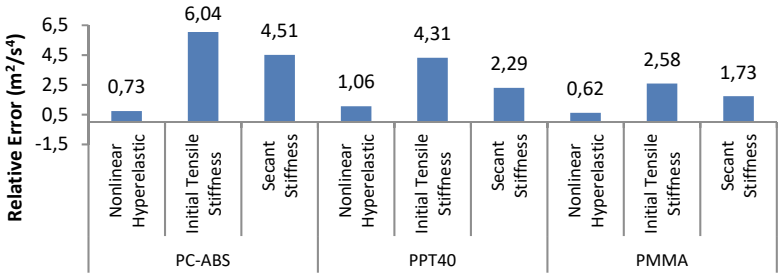

Figure 5: Mean square error of acceleration

It appears that the materials with lower strength had higher mean square error of acceleration for the hyperelastic material model. PMMA material which was the strongest of the three materials had the smallest mean square error followed by PC-ABS and then PPT40 material which had the largest error. The materials with lower strength exhibited stronger nonlinearity and larger errors.

6.2. Statistical analysis of response of the Mooney-Rivlin stiffness based damping matrix

Figs 6-8 show the response statistics of numerically simulated responses based on the Mooney-Rivlin model damping matrix which was compared with that measured using shaker tests. The experimental curve fell within the numerically obtained upper and lower bound response curves for all the three materials. The time histories were divided into two for clarity, (a) represents the first half of the curve and (b) represents the second half. It is worth noting that the result of the experiment was based on only one specimen.

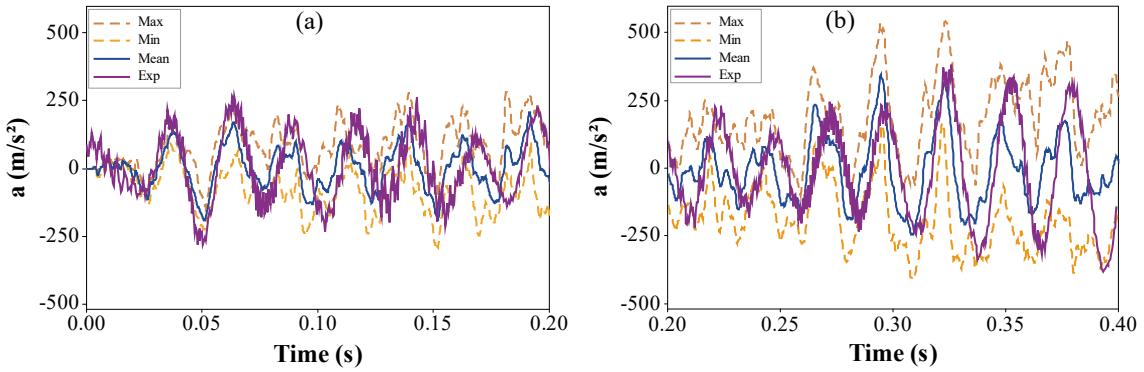

Figure 6: Dynamic response acceleration- PC-ABS - (a) 0 to 0.2sec, (b) 0.2 to 0.4sec

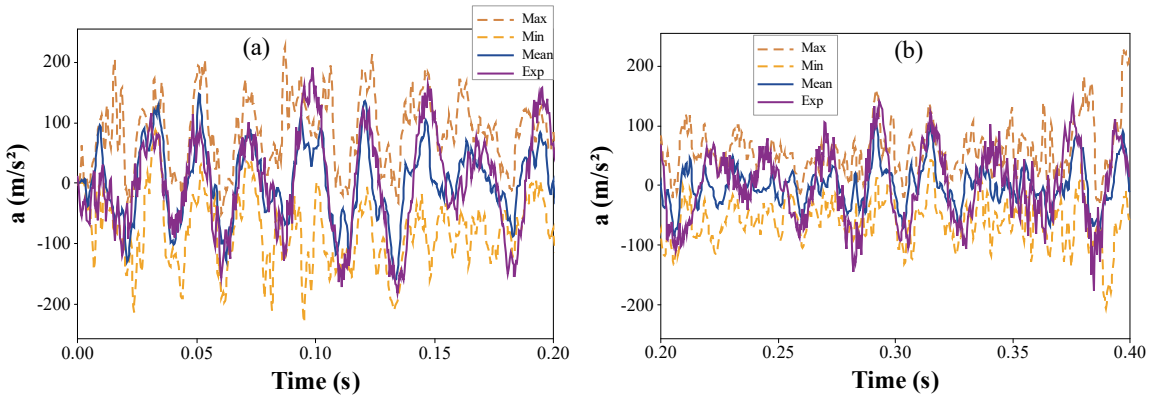

Figure 7: Dynamic response acceleration- PMMA - (a) 0 to 0.2sec, (b) 0.2 to 0.4sec

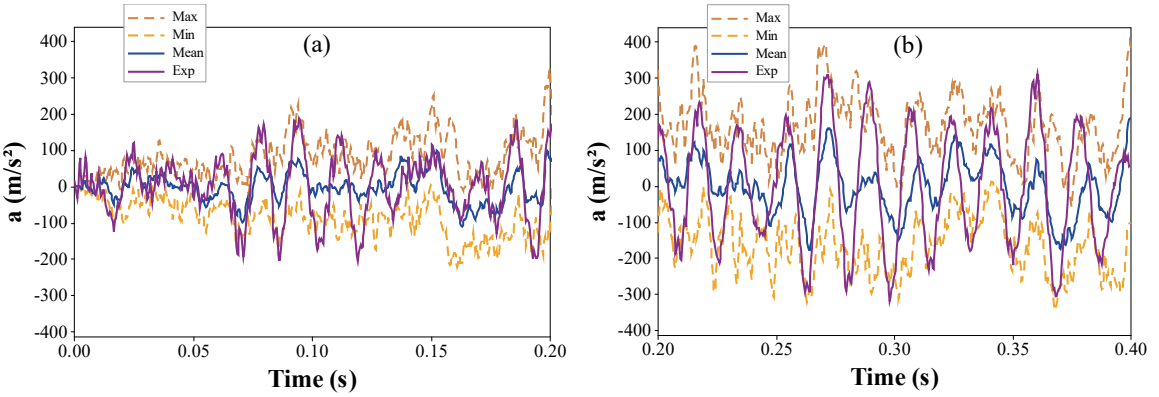

Figure 8: Response acceleration- PPT40 - (a) 0 to 0.2sec, (b) 0.2 to 0.4sec

7. Conclusions

A study on the use of hyperelastic Mooney-Rivlin material model based Rayleigh damping matrix in random vibration response analysis of components of an automotive lamp made of Polycarbonate/Acrylonitrile Butadiene Styrene (PC-ABS), Polymethyl methacrylate (PMMA) and Polypropylene 40% Talc filled (PPT40) materials has been presented. The acceleration response based on nonlinear Mooney-Rivlin stiffness damping matrix was compared to the linear elastic models based stiffness matrices. It was shown that the mean square error of acceleration response for the Mooney-Rivlin model based Rayleigh damping matrix was the least, $0.7(m^2/s^4)$, $1.06(m/s^2)^2$ and $0.62(m^2/s^4)$ for PC-ABS, PMMA and PPT40 respectively. The corresponding values for linear elastic models of initial tensile stiffness and the secant stiffness were $8.3(m^2/s^4)$ and $6.2(m^2/s^4)$ higher than that of Mooney-Rivlin for PC-ABS, $4.2(m^2/s^4)$ and $2.8(m^2/s^4)$ for PMMA and $4.1(m^2/s^4)$ and $2.2(m^2/s^4)$ for PPT40 respectively. The Mooney-Rivlin material model based Raleigh damping matrix was more accurate in modelling the dynamic behaviour of components of nonlinear materials and it represented the manufacturing variabilities more reliably. Therefore, it is essential that nonlinear material stiffness based is used when developing virtual prototype for dynamic response analysis of nonlinear system.

The PMMA material which was the strongest of the three materials had the lowest mean square error of acceleration followed by PC-ABS and then PPT40 material. The materials with lower strength exhibited larger nonlinearity and larger error in the dynamic responses.

Acknowledgements

This research has been funded by Wipac Ltd. The authors would like to acknowledge Albis for providing the PC-ABS test specimens and Plastribution for providing the PPT40 test specimens.

References

British Standards Institution: BS EN ISO 527-2: 2012. Plastics — Determination of tensile properties, Part 2: Test conditions for moulding and extrusion plastics.

International Standard: ISO 16750-3: 2007. Road vehicles — Environmental conditions and testing for electrical and electronic equipment —Part 3: Mechanical loads; Second edition 2007-08-01.

ASTM International: ASTM D638-02a: 2003. Standard Test Method for Tensile Properties of Plastics, Vol 14.02.

Naohiro Nakamura., 2016. Extended Rayleigh Damping Model, Frontiers in Built Environment, doi: 10.3389/fbuil.

Walter D. Pilkey., 2004. Formulas for Stress, Strain, and Structural Matrices, 2nd edition, Wiley & Sons.

C P Okeke, A N Thite, J F Durodola and M T Greenrod., 2017. Hyperelastic polymer material models for robust fatigue performance of automotive LED lamps, Procedia Structural Integrity 5 (2017) 600–607.

Mooney, M., 1940. A theory of large elastic deformation, Journal of applied physics, Vol. 11(9):582-592.

Rivlin, R. S., 1948. Large Elastic Deformations of Isotropic Materials. I. Fundamental Concepts, Philosophical Transactions of the Royal Society of London. Series A, Mathematical and Physical Sciences, Vol. 240, No. 822 (Jan. 13, pp. 459-490.

Dionisio Bernal., 1994. Viscous Damping in Inelastic Structural Response, Journal of Structural Engineering 1994, 120(4): 1240-1254

Finley A. Charney., 2008. Unintended Consequences of Modeling Damping in Structures, Journal of Structural Engineering, Vol. 134, No. 4, April 1, 2008.

Farzin Zareian and Ricardo A. Medina., 2010. A practical method for proper modeling of structural damping in inelastic
plane structural systems, Computers and Structures 88 (2010) 45–53

A. Kareem and K. Gurley., 1996. Damping in structures: its evaluation and treatment of uncertainty, Journal of Wind Engineering and Industrial Aerodynamics 59 (1996) 131-157

P. Jehel, P. Leger and A. Ibrahimbegovic., 2013. Initial vs. tangential stiffness-based Rayleigh damping in inelastic time history seismic analysis, Earthquake Engineering and Structural Dynamics, DOI: 10.1002/eqe.2357.

Kumar, Nomesh., Rao., V. Venkateswara., 2016. Hyperelastic Mooney-Rivlin Model: Determination and Physical Interpretation of Material Constants, MIT International Journal of Mechanical Engineering, Vol. 6, No. 1, J, pp. 43-46 43, ISSN 2230-7680.

Nowark, Z., 2008. Constitutive Modelling and Parameter Identification for Rubber-Like Materials, Engineering Transations, 56, 2,117-157

Pierre Jehel, Pierre Léger and Adnan Ibrahimbegovic., 2014. Initial versus tangent stiffness-based Rayleigh damping in inelastic time history seismic analyses. Earthquake Engineering and Structural Dynamics, Wiley, 2014, 43, pp.467-484.